Clinical Cancer Research

Neddylation Inhibition Activates the Extrinsic Apoptosis Pathway through ATF4–CHOP–DR5 Axis in Human Esophageal Cancer Cells

Ping Chen[1,2], Tao Hu[1], Yupei Liang[2], Pei Li[1], Xiaoyu Chen[1], Jingyang Zhang[1], Yangcheng Ma[1], Qianyun Hao[1], Jinwu Wang[3], Ping Zhang[2], Yanmei Zhang[4], Hu Zhao[4], Shengli Yang[1], Jinha Yu[5], Lak Shin Jeong[5], Hui Qi[6], Meng Yang[6,7,8], Robert M. Hoffman[6,7,8], Ziming Dong[1], and Lijun Jia[2]

Abstract

Purpose: Targeting the protein neddylation pathway has become an attractive anticancer strategy; however, the role of death receptor–mediated extrinsic apoptosis during treatment remained to be determined.

Experimental Design: The activation of extrinsic apoptosis and its role in MLN4924 treatment of human esophageal squamous cell carcinoma (ESCC) were evaluated both *in vitro* and *in vivo*. The expression of the components of extrinsic apoptotic pathway was determined by immunoblotting analysis and downregulated by siRNA silencing for mechanistic studies.

Results: Pharmaceutical or genetic inactivation of neddylation pathway induced death receptor 5 (DR5)–mediated apoptosis and led to the suppression of ESCC in murine models. Mechanistically, neddylation inhibition stabilized activating transcription factor 4 (ATF4), a Cullin-Ring E3 ubiquitin ligases (CRL) substrate. Transcription factor CHOP was subsequently transactivated by ATF4 and further induced the expression of DR5 to activate caspase-8 and induce extrinsic apoptosis. Moreover, the entire neddylation pathway was hyperactivated in ESCC and was negatively associated with patient overall survival.

Conclusions: Our findings highlight a critical role of ATF4–CHOP–DR5 axis-mediated extrinsic apoptosis in neddylation-targeted cancer therapy and support the clinical investigation of neddylation inhibitors (e.g., MLN4924) for the treatment of ESCC, a currently treatment-resistant disease with neddylation hyperactivation. *Clin Cancer Res; 22(16); 4145–57. ©2016 AACR.*

Introduction

Protein posttranslational modifications play a crucial role in the regulation of tumorigenesis and tumor progression. Neddylation is a novel type of posttranslational modification that adds the ubiquitin-like molecule NEDD8 to substrate proteins and thus regulates their function (1–3). This process is catalyzed by a cascade comprising the NEDD8-activating enzyme E1 (NAE, NAE1 and UBA3 heterodimer), NEDD8-conjugating enzyme E2, and substrate-specific NEDD8-E3 ligases (1–3). The best known substrates of neddylation are cullin family proteins, the essential subunits of multiunit Cullin-RING E3 ubiquitin ligases (CRL) whose dysfunction leads to tumorigenesis and tumor progression (1–3). NEDD8 conjugation also regulates the function of several other important cancer-related proteins, including oncoproteins [e.g., Mdm2 (4), HuR (5), and Smurf1 (6)] and tumor suppressors [e.g., p53 (4), pVHL (7), and TGFβ type II receptor (8)]. Moreover, the entire neddylation pathway, including NEDD8-activating enzyme E1, NEDD8-conjugating enzyme E2, and global neddylation of substrates, is reported to be hyperactivated in several human cancers and associated with disease progression, such as worse patient overall survival (3, 6, 9, 10). These findings highlight a pivotal role of neddylation in carcinogenesis and tumor progression and support to develop neddylation as an attractive anticancer target.

Targeting neddylation pathway has been recently demonstrated as an attractive anticancer strategy, evidenced by the efficacy of the NAE inhibitor MLN4924, a first-in-class anticancer agent, in a multitude of preclinical studies (1–3, 11–19). Currently, MLN4924, used as a single agent or in combination with traditional chemotherapeutics, is under investigation in quite a few of phase I/II clinical trials (http://www.clinicaltrials.gov) and has

[1]College of Basic Medical Sciences, Zhengzhou University; Collaborative Innovation Center of Henan Province for Cancer Chemoprevention, Zhengzhou, China. [2]Cancer Institute, Fudan University Shanghai Cancer Center; Collaborative Innovation Center of Cancer Medicine; Department of Oncology, Shanghai Medical College, Fudan University, Shanghai, China. [3]Department of Pathology, Linzhou Cancer Hospital, Linzhou, China. [4]Department of Clinical Laboratory, Huadong Hospital; Shanghai Key Laboratory of Clinical Geriatric Medicine; Research Center on Aging and Medicine, Fudan University, Shanghai, China. [5]College of Pharmacy, Seoul National University, Seoul, Korea. [6]AntiCancer Biotech (Beijing) Co., Ltd., Beijing, China. [7]Department of Surgery, University of California, San Diego, California. [8]AntiCancer, Inc., San Diego, California.

Note: Supplementary data for this article are available at Clinical Cancer Research Online (http://clincancerres.aacrjournals.org/).

P. Chen and T. Hu contributed equally to this article.

Corresponding Authors: Lijun Jia, Cancer Institute, Fudan University Shanghai Cancer Center, 270 Dongan Rd, Shanghai 200032, China. Phone: 86-13585779708; Fax: 86-21-54237751; E-mail: ljjia@fudan.edu.cn; Ziming Dong, College of Basic Medical Sciences, Zhengzhou University; Collaborative Innovation Center of Henan Province for Cancer Chemoprevention, Zhengzhou 450001, China. Phone: 86-371-67739523; E-mail: dongzm@zzu.edu.cn; or Ping Chen, Phone: 86-13460203714; E-mail: zzdx_chenping@zzu.edu.cn

doi: 10.1158/1078-0432.CCR-15-2254

Translational Relevance

Esophageal cancer is one of the most deadly human cancers of the digestive system. Although great efforts have been made to develop novel anti-ESCC strategies, few achievements have been obtained in the effective treatment of ESCC. In this study, we report that the entire neddylation pathway is hyperactivated in ESCC and negatively associated with overall survival of ESCC patients, implying that neddylation is an attractive anticancer target of ESCC. Moreover, we find that pharmaceutical or genetic inactivation of neddylation pathway induces ATF4–CHOP–DR5 axis-mediated extrinsic apoptosis and leads to significant suppression of human ESCC tumors in murine model. Our findings highlight a critical role of the overactivated neddylation pathway in the development of esophageal cancer and, more importantly, support the future clinical investigation of neddylation inhibitors (e.g., MLN4924) for the treatment of ESCC, a currently treatment-resistant disease.

exhibited promising clinical activity in both advanced solid tumors and relapsed/refractory multiple myeloma or lymphoma (18, 19). Mechanistically, MLN4924 blocks cullin neddylation, inactivates CRL, induces the accumulation of tumor-suppressive CRL substrates, and eventually causes DNA re-replication stress/DNA damage, cell-cycle arrest, senescence, or apoptosis in a cell-type–dependent manner (1–3, 11–14, 20–22). Although induction of intrinsic (mitochondrial) apoptosis by MLN4924 has been reported previously (3, 12, 22), whether MLN4924 activates the extrinsic (death receptor–mediated) apoptosis in human cancer cells is largely unknown.

Esophageal cancer is the fourth most common cancer of the digestive system and the sixth leading cause of cancer-related deaths in the world (23). Esophageal squamous cell carcinoma (ESCC) is a major histologic subtype among all types of the esophageal tumors (23). Despite clinical advances in the development of various therapeutic approaches, the overall 5-year survival rate for esophageal cancer patients is still very poor (23). Major limitations to the treatment of ESCC include high toxicity of traditional chemotherapeutics and acquired therapeutic resistance (24). Therefore, there is an urgent need to identify new anti-ESCC molecular targets and develop novel therapeutic strategies for the treatment of esophageal cancer.

Here, for the first time, we reported that targeting hyperactivated neddylation pathway pharmaceutically or genetically triggered ATF4–CHOP–death receptor 5 (DR5) axis-mediated extrinsic apoptosis to significantly inhibit the growth of human ESCC tumors. Our findings not only reveal a previously unrecognized mechanism for the cytotoxic effects of neddylation inhibition but also provide a solid evidence for clinical investigation of neddylation inhibitors (e.g., MLN4924) for the treatment of ESCC.

Materials and Methods

Cell lines, culture, and reagents

Human ESCC cell lines EC1, EC109, Kyse450, Kyse30, and Kyse510 were routinely cultured in Dulbecco's Modified Eagle's Medium (Hyclone), containing 10% FBS (Biochrom, AG) and 1% penicillin–streptomycin solution, at 37°C with 5% CO_2. MLN4924 was synthesized and prepared as previously described (3, 25, 26).

Cell viability and clonogenic survival assay

Cells were seeded in 96-well plates (3×10^3 cells per well) and treated with DMSO or MLN4924. Cell proliferation was determined using the ATPLite Luminescence Assay Kit (PerkinElmer) according to the manufacturer's protocol.

For the clonogenic assay, 500 cells were seeded into 60-mm dishes in triplicate, treated with DMSO or MLN4924, and then incubated for 12 days. The colonies were fixed, stained, and counted under an inverted microscope (Olympus). Colonies comprising 50 cells or more were counted.

Detection of apoptosis and activity assays of CASP8 and CASP3

Cells were treated with the indicated concentration of MLN4924 for 72 hours. Apoptosis was determined with the Annexin V-FITC/PI Apoptosis Kit (BioVision, Inc.) according to the manufacturer's instructions. The activities of CASP8 and CASP3 were measured using the CaspGLOW assay Kit (BioVision, Inc.) according to the manufacturer's instructions.

Immunoblotting

Esophageal cancer and adjacent esophageal tissues were collected and analyzed for the expression of NEDD8-conjuagated protein, NAE1, UBA3, and UBC12. Cell lysates were prepared for immunoblotting (IB) analysis, with antibodies against cleaved caspase-8 (CASP8), CHOP, ATF4, Apoptosis Antibody Sampler Kit, Pro-Apoptosis Bcl-2 Family Antibody Sampler Kit, Pro-Survival Bcl-2 Family Antibody Sampler Kit, IAP Family Antibody Sampler Kit (Cell Signaling Technology), Cullin1 (Santa Cruz Biotechnology), DR5 (Abcam Trading Company Ltd), tubulin (Likun Trade Co.), and Noxa (Millipore).

Evaluation of mitochondrial membrane depolarization

Kyse450 and EC1 cells were treated with DMSO or MLN4924. Mitochondrial membrane depolarization was detected with the mitochondrial membrane potential assay Kit with JC-1 according to the manufacturer's protocol (Yeasen Inc). The data were acquired and analyzed by flow cytometry as described previously (26).

Gene silencing using siRNA

Kyse450 and EC1 cells were transfected with siRNA oligonucleotides, synthesized by RIBOBIO using Lipofectamine 2000. The sequences of the siRNA are as follows: siCASP9 (27): GAUGCCUGGUUGCUUUAAU; siCASP8 (27): UGGAUUUGCUGAUUACCUA; siNoxa (28): GUAAUUAUUGACACAUUUC; siBid (29): AAGAAGACAUCAUCCGGAAUA; siDR5 (30): AAGACCCUUGUGCUCGUUGUC; siCHOP (31): GCCUGGUAUGAGGACCUGC; siATF4 (31): GCCUAGGUCUCUUAGAUGA; siUBA3 (2): CUGCCUGGAAUGACUGCUUAA; siNAE1 (10): GGGUUGUGCUUUAGUCUGU; and siTRAIL (27): CAAGUUAUCCUGACCCUAU.

RNA extraction and qPCR

Total RNA was extracted using the Ultrapure RNA Kit (CWbiotech). RNA (1.0 μg) was purified and reversely transcribed by PrimeScript RT Master (Takara) following the manufacturer's instructions. The cDNA was quantified by real-time quantitative

PCR using SYBR Green Real-Time PCR Master Mixes (Applied Biosystems) and a Real-time PCR system (Applied Biosystems) according to the manufacturer's instructions. For each sample, the mRNA abundance was normalized to the amount of GAPDH. Primers are as follows: Noxa: forward, 5′-GGAGATGCCTGGGAAGA-3′, reverse, 5′-TTCTGCCGGAAGTTCAGT-3′; CHOP: forward, 5′-AGCCAAAATCAGAGCTGGAA-3′, reverse, 5′-TGGATCAGTCTGGAAAAGCA-3′; DR5: forward, 5′-CCAGCAAATGAAGGTGATCC-3′, reverse, 5′-GCACCAAGTCTGCAAAGTCA-3′; ATF4: forward, 5′-GCTAAGGCGGGCTCCTCCGA-3′, reverse, 5′-ACCCAACAGGGCATCCAAGTCG-3′; GAPDH: forward, 5′-AAAGGGTCATCATCTCTG-3′, reverse, 5′-GCTGTTGTCATACTTCTC-3′.

Cell surface expression of DR5 measured by flow cytometry

Cells were treated with MLN4924 (0.6 μmol/L) or DMSO, collected, and then stained for DR5 cell surface expression for FACS analysis using purified mouse monoclonal FITC-conjugated anti-DR5 antibody (Abcam Trading Company Ltd) or its isotype IgG (Santa Cruz Biotechnology) according to standard procedures.

In vivo ubiquitination assay

To determine the effect of MLN4924 on ATF4 ubiquitination, cells were pretreated with MG132 and starved for 12 hours, and then cells were treated with MLN4924, along with DMSO control for another 12 hours, followed by serum addition for 2 hours. Cells were extracted and subjected to immunoprecipitation (IP) with anti-ATF4 Ab and IB with anti-ubiquitin Ab.

Subcutaneous transplantation tumor model of human esophageal cancer and treatment

A subcutaneous transplantation tumor model of human esophageal cancer was established using EC1-GFP or Kyse450 esophageal cancer cells (32). The tumor-bearing mice were randomized into 2 groups and treated with 10% 2-hydroxypropyl-β-cyclodextrin (HPBCD; Sigma) or MLN4924 (45 mg/kg) twice a day, on a 3-days-on/2-days-off schedule as previously described (25, 26). Whole-body images were acquired using the Olympus OV100 imaging system twice a week as described (3, 25, 26, 33). Tumor size was determined by caliper measurement. The tumor volume was calculated using the ellipsoid volume formula (Length $\times$ Width^2/2). Tumor tissues were harvested, photographed, and weighed. Protein expression of tumor tissues was evaluated by IB analysis using specific antibodies as indicated. Animal experiments were performed in accordance with animal protocols approved by the Institutional Animal Care and Use Committee of AntiCancer Biotech (Beijing) Co., Ltd.

Immunohistochemistry staining of human esophageal cancer tissue arrays

Human esophageal cancer tissue arrays were purchased from Shanghai Outdo Biotech Co. Ltd. IHC staining was conducted with NAE1 (Sigma), UBA3, UBC12, and NEDD8 antibodies (Cell Signaling Technology). The detailed clinicopathologic characteristics of ESCC patients are listed in Supplementary Tables S1 and S2 for statistical analysis. The tissue array sections (4 μm) were dehydrated and subjected to peroxidase blocking. Primary antibodies were added and incubated at 4°C overnight, followed by staining with a GTVisionTM III Detection System/Mo&Rb (Gene Tech Company Limited). The slides were counterstained with hematoxylin. The stained slides were observed under microscopy, and images were acquired. Overall survival was calculated using the Kaplan–Meier analysis and compared with the log-rank test.

Collection of esophageal cancer tissues and clinicopathologic characteristics of patients

Fresh primary esophageal cancer tissues and adjacent esophageal tissues were collected from 10 ESCC patients undergoing resection at the Linzhou Cancer Hospital (Linzhou, Henan, China) from July 2012 to September 2014. Histologic diagnosis and tumor–node–metastasis stages of cancers were determined in accordance with the American Joint Committee on Cancer manual criteria for esophageal cancer. Written informed consent regarding tissue and data used for scientific purposes was obtained from all participated patients. The study was approved by the Research Ethics Committee of Linzhou Cancer Hospital.

Statistical analysis

The statistical significance of differences between groups was assessed using GraphPad Prism5 software. The *t* test was used for the comparison of parameters between groups. The Mann–Whitney test was used for data that are not of normal distribution by SPSS software. For all tests, three levels of significance (*, $P < 0.05$; **, $P < 0.01$; ***, $P < 0.001$) were applied.

Results

The neddylation pathway is hyperactivated in ESCC and predicts diminished survival in ESCC patients

To investigate the activation status of neddylation pathway in esophageal cancer, we firstly examined the expression levels of global protein neddylation by IHC staining of the tissue arrays derived from human ESCC, which contain 95 pairs of primary tumor versus adjacent normal tissues. Based on staining intensity, we classified the samples into five groups with increasing staining intensity from the weakest (±, group 1) to the strongest (++++, group 5; Fig. 1A). Staining-intensity analysis demonstrated that global protein neddylation was substantially elevated in ESCC tissues when compared with their corresponding adjacent normal tissues ($P < 0.01$; Fig. 1B), which was confirmed by IB analysis (Supplementary Fig. S1A). Furthermore, the elevated protein neddylation is negatively correlated with 5-year overall survival rate of ESCC patients determined by the Kaplan–Meier analysis ($P = 0.033$, log-rank test; Fig. 1C).

Considering that global protein neddylation was elevated in tumor tissues (Fig. 1A–C and Supplementary Fig. S1A), we further hypothesized that key components of neddylation pathway, including NEDD8-activating enzyme E1 (NAE, NAE1, and UBA3 heterodimer) and NEDD8-conjugating enzyme E2 (UBC12), may also be overexpressed in tumor tissues. Indeed, NAE1, UBA3, and UBC12 were observed to be overexpressed in ESCC tissues compared with adjacent normal esophageal tissues (Supplementary Fig. S1B–S1D). These findings provided the rationality for the further evaluation of overactivated neddylation pathway as a potential anti-ESCC target.

Neddylation inhibition by MLN4924 suppresses the growth of ESCC cells and activates the extrinsic apoptosis pathway

To explore the possibility of neddylation inhibition as an anticancer strategy in ESCC, we first evaluated the anticancer

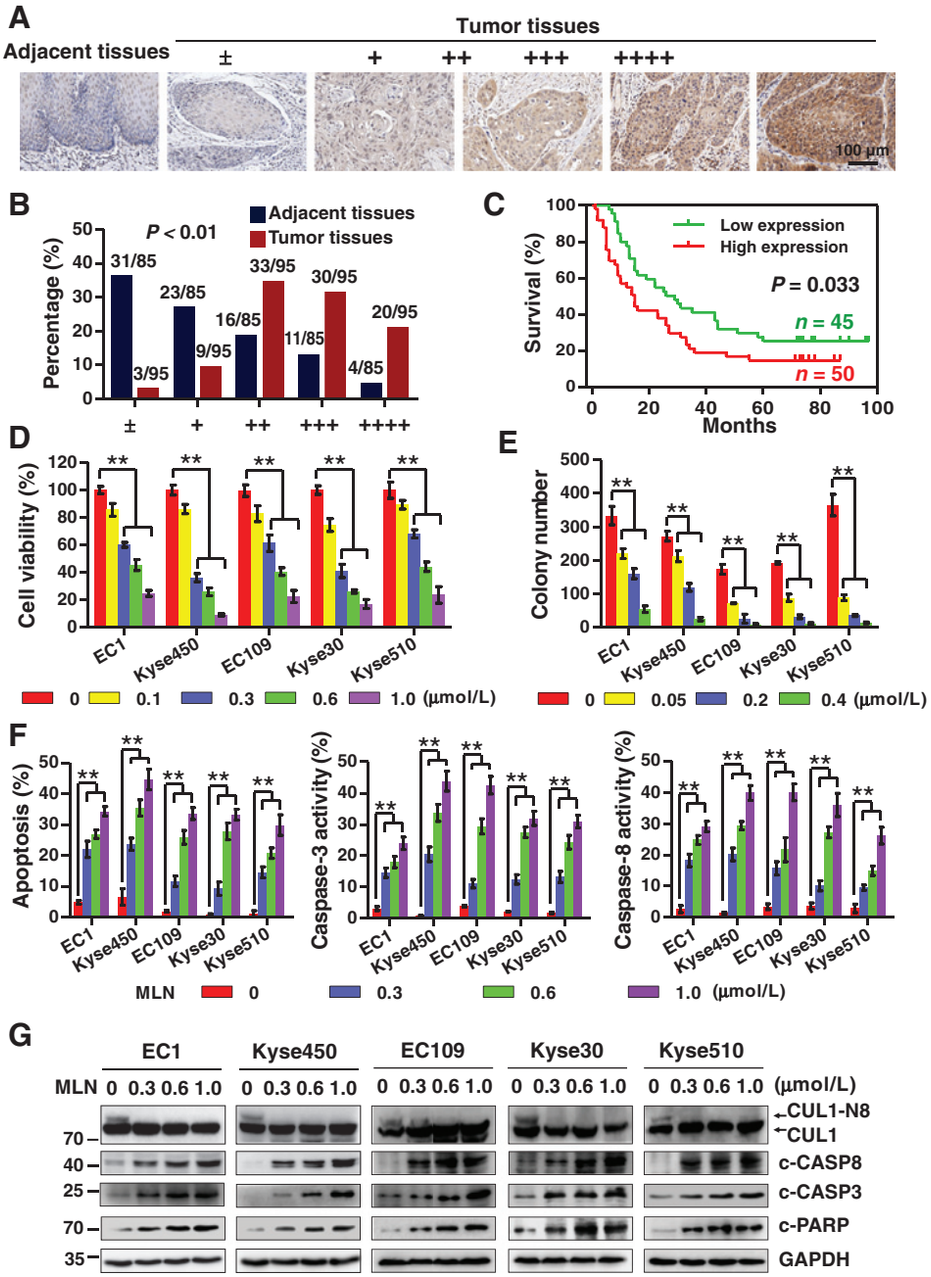

Figure 1.

Inhibition of overactivated neddylation pathway inhibits proliferation and activates extrinsic apoptosis of human esophageal cancer cells. **A–C**, hyperactivation of the global neddylation pathway in ESCC. **A,** IHC staining of human ESCC tissues arrays using NEDD8-specific antibodies. Based on staining intensity, we classified the samples into five groups with increasing staining intensity from the weakest (±, group 1) to the strongest (++++, group 5). **B,** classification of tumor samples according to the staining intensity of NEDD8 ($n = 95$). Statistical analysis of staining intensity by the Mann–Whitney test showed that there are significant differences between tumor and their adjacent tissues ($P < 0.01$). **C,** Kaplan–Meier curves for the overall survival rate of patients with ESCC according to the expression of NEDD8 ($P = 0.033$, log-rank test). Groups 1 to 3 were designated as low expression, and Groups 4 to 5 were designated as high expression. **D,** efficacy of MLN4924 on the viability of ESCC cells EC1, EC109, Kyse450, Kyse510, and Kyse30. Cells were treated with the indicated concentrations of MLN4924 for 72 hours, and viability was assessed with the ATPLite assay. **E,** efficacy of MLN4924 on clonogenic survival. ESCC cells EC1, EC109, Kyse450, Kyse510, and Kyse30 were treated with MLN4924 at the indicated concentrations for 12 days, and then fixed, stained, and counted as described in Materials and Methods. **F,** MLN4924 induced apoptosis and activation of CASP3 and CASP8. Cells were treated with MLN4924 for 72 hours. Apoptosis was determined by Annexin V–FITC/PI double-staining analysis (left); CASP3 (middle) and CASP8 (right) activity was analyzed with FACS. All data were representative of at least three independent experiments (**, $P < 0.01$; $n = 3$; error bar, SD). **G,** treatment with MLN4924 suppressed cullin1 neddylation (CUL1-N8) and increased the cleavage of CASP8, CASP3, and PARP. ESCC cell lines were treated with MLN4924 for 72 hours, and cell lysates were assessed by IB with specific antibodies against cullin1, cleaved CASP8, CASP3, or PARP.

efficacy of MLN4924 on ESCC cell lines EC1, EC109, Kyse450, Kyse30, and Kyse510. We found that MLN4924 induced a dose-dependent inhibition of cell proliferation (Fig. 1D) and colony formation (Fig. 1E) of ESCC cells. MLN4924 treatment induced a significant increase in Annexin V–positive cells (Fig. 1F, left) and caspase-3 (CASP3)–activated cells (Fig. 1F, middle), indicating that MLN4924 triggered apoptosis in ESCC cell lines. In order to determine whether MLN4924 triggers the extrinsic apoptosis pathway, the activity of CASP8 was measured. As shown in Fig. 1F (right), MLN4924 induced a significant increase in CASP8-activated cells. Similarly, MLN4924 significantly induced the cleavage of CASP8, CASP3, and PARP (Fig. 1G). These results suggest that MLN4924 triggered extrinsic apoptosis in ESCC cells.

Activation of CASP8 and the cleavage of Bid are required for MLN4924-induced apoptosis

Our results presented above showed that MLN4924 significantly induced the activation of CASP8 (Fig. 1F and G) which plays a central role in the induction of the extrinsic apoptosis pathway. Next, we determined the role of the extrinsic apoptosis pathway in MLN4924-induced apoptosis by downregulating the expression of CASP8 via siRNA in EC1 and Kyse450, two representative ESCC cell lines. As shown in Fig. 2A, knockdown of CASP8 significantly blocked MLN4924-induced apoptosis, indicating a critical role of CASP8 activation in MLN4924-induced apoptosis. As a classical mediator of the extrinsic apoptosis pathway, CASP8 activation may also trigger the intrinsic apoptosis pathway by cleaving BH3 interacting domain death agonist (Bid) and releasing its COOH-terminal fragment (tBid) which translocate to mitochondria where it triggers cytochrome c release and induces intrinsic apoptosis.

To test this hypothesis, we first determined the expression of tBid and cleaved CASP9, as classical markers of the intrinsic apoptosis pathway. The expression of tBid and cleaved CASP9 was significantly induced by MLN4924 (Fig. 2B). Meanwhile, MLN4924 induced the loss of mitochondrial membrane potential ($\Delta\psi m$), another classical marker of the activation of intrinsic apoptosis (Fig. 2C), which further indicated the induction of intrinsic apoptosis. To determine the role of CASP8/tBid axis in MLN4924-induced apoptosis, the expression of CASP8 and Bid was downregulated via siRNA silencing, respectively. As shown in Fig. 2D, downregulation of CASP8 significantly attenuated the induction of tBid and cleaved PARP. Moreover, Bid downregulation significantly reduced MLN4924-induced apoptosis (Fig. 2E) and CASP3 activation (Fig. 2F) as well as the cleavage of PARP (Fig. 2G). These findings collectively demonstrated that MLN4924-induced CASP8 activation also triggered the intrinsic apoptosis pathway by cleaving Bid to release tBid, a critical effector linking the extrinsic apoptosis to the intrinsic apoptosis.

The induction of DR5 plays a critical role for CASP8 activation upon MLN4924 treatment

To explore the mechanism for the activation of extrinsic (death receptor–mediated) apoptosis upon MLN4924 treatment, the expression of death receptor family members, including classical apoptosis-inducing ligands and their receptors (death receptors) as well as signal regulators of the extrinsic apoptosis pathway, was first determined (Fig. 3A and Supplementary Fig. S2A). Among these proteins, MLN4924 significantly induced the expression of death receptor DR5 both at protein and mRNA levels (Fig. 3A), which was further confirmed by FACS analysis of the expression of cell surface DR5 (Fig. 3B). Collectively, these findings indicated that the transactivation of DR5 was responsible for the induction of extrinsic apoptosis upon MLN4924 treatment.

To further define the role of DR5 expression in MLN4924-induced CASP8 activation and apoptosis, the expression of DR5 was downregulated by siRNA silencing in MLN4924-treated cells. DR5 knockdown significantly reduced the induction of apoptosis (Fig. 3C) and attenuated the activity of CASP8 (Fig. 3D) and CASP3 (Fig. 3E). Moreover, DR5 downregulation also significantly reduced the cleavage of CASP8, Bid, and PARP in MLN4924-treated cells (Fig. 3F). These results highlighted a critical role of DR5 in MLN4924-induced CASP8 activation and extrinsic apoptosis.

DR5 activation could be triggered upon binding to its cognate ligand TRAIL (TNF-related apoptosis-inducing ligand). To examine whether DR5-induced apoptosis upon MLN4924 treatment is TRAIL-dependent, TRAIL expression was downregulated by siRNA silencing. We found that knockdown of TRAIL could not rescue DR5-induced apoptosis upon MLN4924 treatment, as determined by measuring the percentage of Annexin V–positive cells (Supplementary Fig. S3A), CASP3-activated cells (Supplementary Fig. S3B) as well as the expression of cleaved PARP (Supplementary Fig. S3C). These results indicate that MLN4924 acts on DR5-mediated apoptosis independent of TRAIL.

DR5 is transactivated by activating transcription factor 4/CHOP axis

Previous studies demonstrated that activating transcription factor 4 (ATF4) serves as a substrate of CRL/$SCF^{\beta Trcp}$ ubiquitin ligase (21, 34, 35), and transcription factor CHOP, a classical downstream target of ATF4, can regulate the transactivation of DR5 (36–38). Based on this, we hypothesized that MLN4924 may induce ATF4 accumulation due to the inactivation of CRL/$SCF^{\beta Trcp}$ ubiquitin ligase which requires nedd8 conjugation to its essential subunit cullins for activation, and therefore transactivates CHOP and DR5 to activate extrinsic apoptosis. To test this hypothesis, we first examined the expression of ATF4 and CHOP upon MLN4924 treatment. We found that MLN4924 indeed induced the expression of ATF4 and CHOP in both EC1 and Kyse450 cells (Fig. 4A). MLN4924 significantly increased the mRNA level of CHOP, whereas it had little effect on the transcription of ATF4 (Supplementary Fig. S4A). Furthermore, after blocking protein synthesis with cycloheximide, we observed that the protein stability and half-life of ATF4 were dramatically increased by MLN4924 treatment (Fig. 4B). Similarly, treatment of cells with MG-132, a classical proteasome inhibitor, also dramatically extended the half-life of ATF4 when compared with control cells (Supplementary Fig. S4B). By performing protein ubiquitination assay, we further found that MLN4924 significantly inhibited the polyubiquitination modification of ATF4 (Supplementary Fig. S4C). These findings collectively demonstrate that the proteasome-dependent degradation of ATF4 was blocked upon the inactivation of CRL/$SCF^{\beta Trcp}$ ubiquitin ligase by MLN4924.

Next, we determined whether the induction of ATF4 and CHOP expression was responsible for MLN4924-induced DR5 expression. We found that ATF4 knockdown significantly inhibited the transactivation of both CHOP and DR5 (Fig. 4C and Supplementary Fig. S5A). Similarly, CHOP knockdown suppressed the

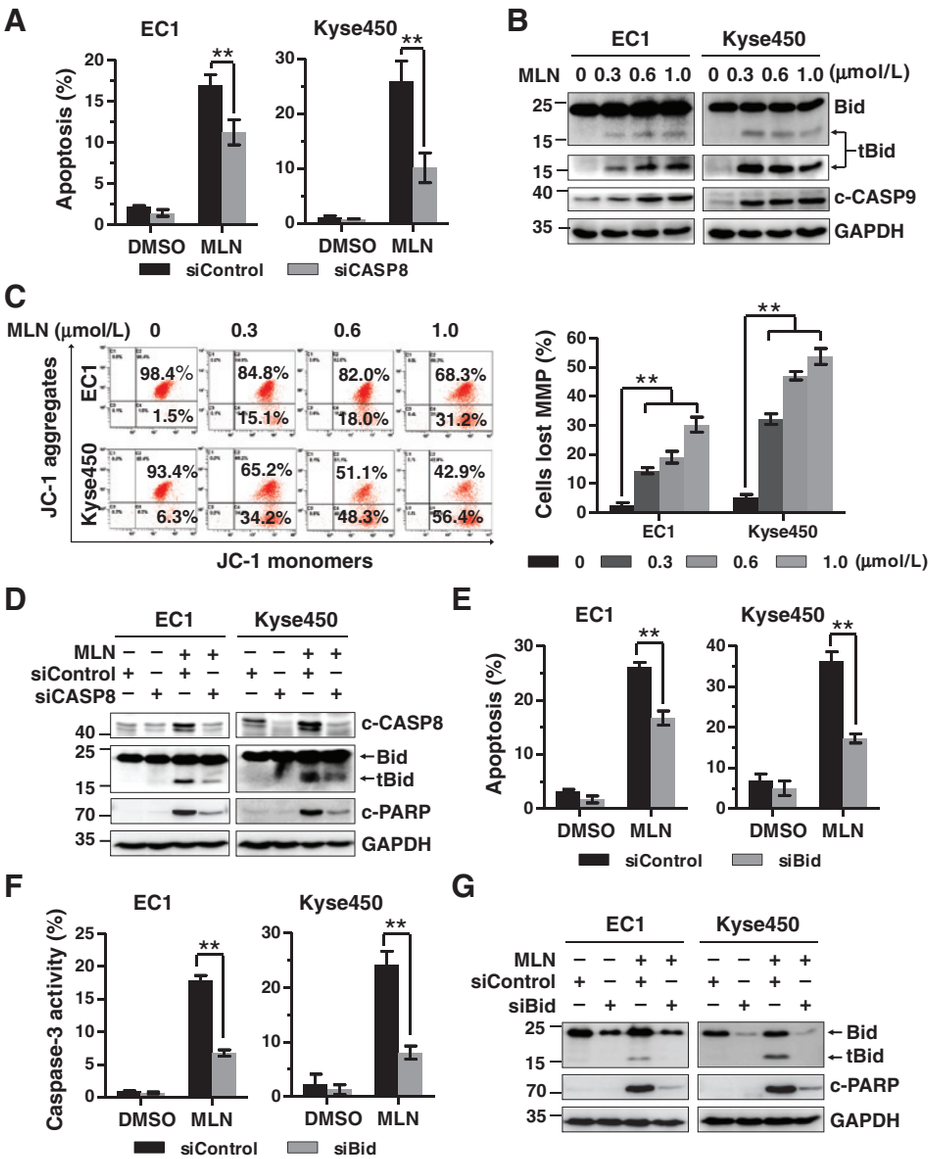

Figure 2.

CASP8 activation and Bid cleavage contribute to MLN4924-mediated apoptosis. **A,** knockdown of CASP8 expression with siRNA partially inhibited apoptosis induced by MLN4924. Kyse450 and EC1 cells were transfected with control or CASP8 siRNA for 48 hours and then treated with 0.6 μmol/L MLN4924 for 48 hours. Apoptosis induction was quantified by Annexin V–FITC/PI double-staining analysis. **B,** CASP8 activation triggered the intrinsic apoptosis pathway by cleaving Bid. EC1 and Kyse450 cells were treated with the indicated concentrations of MLN4924 for 72 hours, and then cleaved Bid and CASP9 were detected by IB analysis. **C,** MLN4924 caused mitochondrial membrane depolarization. Kyse450 and EC1 cells were treated with MLN4924 as indicated. Mitochondrial membrane depolarization was detected with the Mitochondrial Membrane Potential Assay Kit with JC-1, according to the manufacturer's protocol. Cells with intact mitochondria displayed high red fluorescence and appeared in the upper right quadrant of the scatterplots. In contrast, cells that had lost mitochondrial membrane potential (MMP) displayed high green and low red fluorescence and appeared in the lower right quadrant (left). Percentage of cells that had lost mitochondrial membrane potential is shown in right plot. **D,** downregulation of CASP8 significantly attenuated the cleavage of Bid and PARP. Kyse450 and EC1 cells were transfected with control or CASP8 siRNA for 48 hours and then treated with 0.6 μmol/L MLN4924 for 48 hours. Knockdown efficiency and cleavage of Bid or PARP were assessed by IB analysis. **E–G,** Bid knockdown attenuated apoptosis induced by MLN4924. Kyse450 and EC1 cells were transfected with control or Bid siRNA and then treated with 0.6 μmol/L MLN4924 for 48 hours. Apoptosis induction was quantified by Annexin V–FITC/PI double-staining analysis (**E**) or CASP3 activity analysis with FACS (**F**). Knockdown efficiency and cleaved PARP were assessed by IB analysis (**G**). All data were representative of at least three independent experiments (**, $P < 0.01$; $n = 3$; error bar, SD).

transactivation of DR5 (Fig. 4D and Supplementary Fig. S5B). ATF4 or CHOP knockdown also significantly inhibited the expression of DR5 and reduced the cleavage of CASP8, Bid, and PARP (Fig. 4E). Moreover, knockdown of ATF4 or CHOP remarkably attenuated the MLN4924-induced apoptosis and the activation of CASP8 and CASP3 (Fig. 4F). Together, these findings convincingly

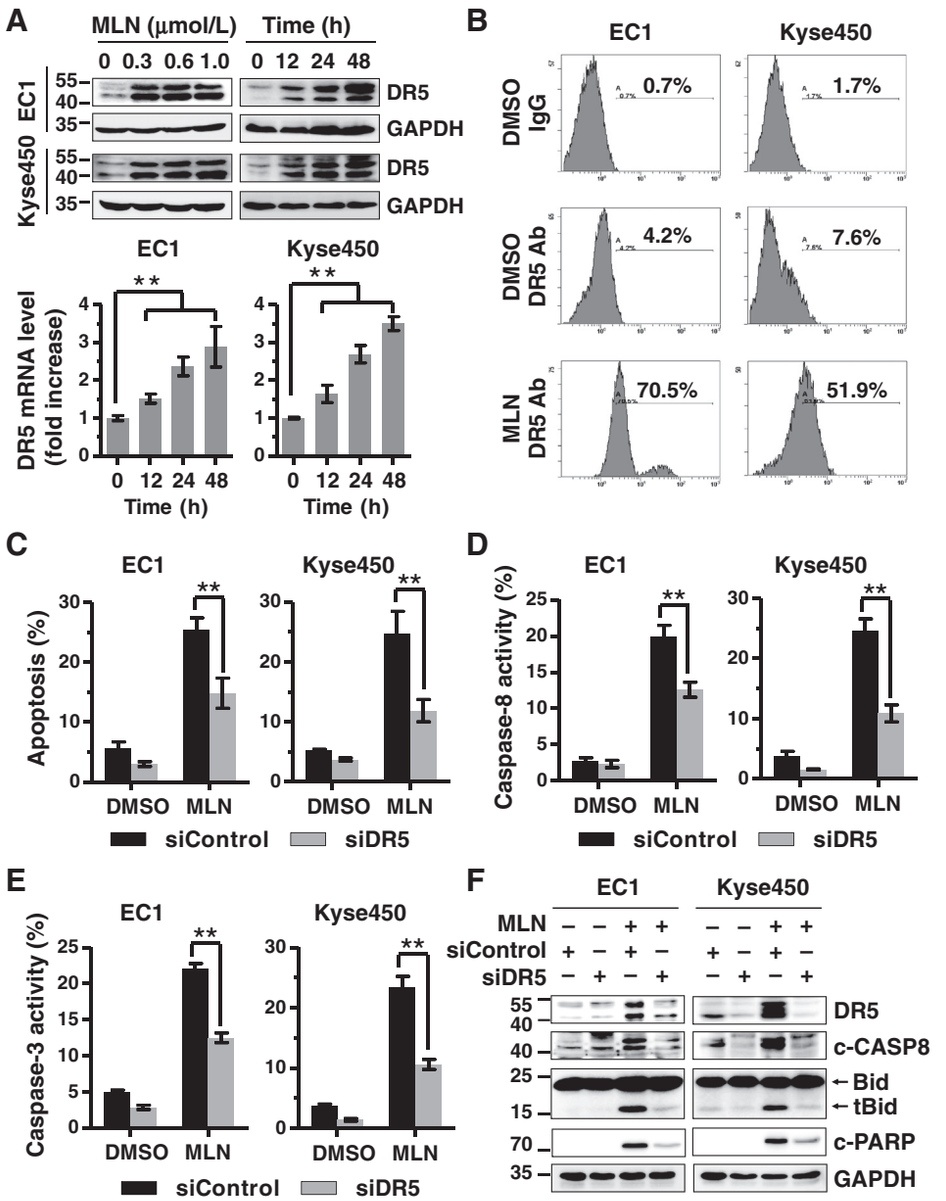

Figure 3.
DR5 upregulation is critical for CASP8 activation induced by MLN4924 in ESCC cells. **A,** MLN4924 increased both the protein and mRNA level of DR5. Cells were treated with MLN4924 with the indicated doses and time points. Cell extracts were prepared for IB analysis of DR5 (top). Total RNAs were isolated from ESCC cells treated with 0.6 μmol/L MLN4924 for the indicated time points. qPCR analysis of DR5 and GAPDH was performed (bottom). **B,** the expression of cell surface DR5. Kyse450 and EC1 cells were treated without or with 0.6 μmol/L MLN4924 for 24 hours. Cells were subjected to FACS analysis to measure cell surface expression of DR5. **C–F,** DR5 upregulation was critical for CASP8-dependent apoptosis induced by MLN4924 in ESCC cells. Kyse450 and EC1 cells transfected with the control siRNA or DR5 siRNA were further treated with 0.6 μmol/L MLN4924 for 48 hours. Apoptosis was quantified by Annexin V–FITC/PI double-staining analysis (**C**); by enzymatic activity assays for CASP8 (D); or CASP3 (**E**) with FACS. Knockdown efficiency, DR5-mediated CASP8 activation, and Bid and PARP cleavage were assessed by IB analysis (**F**). All data were representative of at least three independent experiments (**, $P < 0.01$; $n = 3$; error bar, SD).

demonstrated that the ATF4–CHOP axis was responsible for the induction of DR5 and CASP8-mediated extrinsic apoptosis.

ATF4 also regulates the expression of proapoptotic protein Noxa and contributes to the induction of intrinsic apoptosis

Our aforementioned results indicated that MLN4924 also triggered the intrinsic apoptosis (Fig. 2). To determine the potential role of the activation of intrinsic apoptosis, CASP9 was downregulated via siRNA silencing, and its effect on MLN4924-induced apoptosis was determined. CASP9 downregulation significantly attenuated the apoptotic induction (Fig. 5A, left plots) and reduced the cleavage of CASP3 and PARP (Fig. 5A, right plots) upon MLN4924 treatment. To further define the potential mechanisms for MLN4924-induced intrinsic apoptosis, the expression of classical proapoptotic proteins (Noxa, Bad, Bak, Bax, Puma, and Bim) and antiapoptotic proteins (BCL-2, BCL-XL, Livin, MCL1, c-IAP1, and XIAP) was determined in Kyse450 and EC1 cells after MLN4924 treatment (Fig. 5B and Supplementary Fig. S2B). Among these proteins, the proapoptotic protein Noxa was significantly induced in both cell lines (Fig. 5B, left). Mechanistic studies demonstrated that the expression of Noxa was regulated at mRNA level (Fig. 5B, right). Moreover, Noxa downregulation via siRNA silencing remarkably suppressed MLN4924-induced apoptosis, as evidenced by (i) the decrease of Annexin V–positive (Fig. 5C, left plots) and CASP3-activated (Fig. 5C, right plots) cells; and (ii) the reduction of cleaved CASP3 and PARP (Fig. 5D). These findings highlighted a pivotal role of Noxa transactivation in MLN4924-induced intrinsic apoptosis.

Based on the previous findings that Noxa could be transactivated by ATF4 (39, 40) which was stabilized by MLN4924 (Fig. 4A

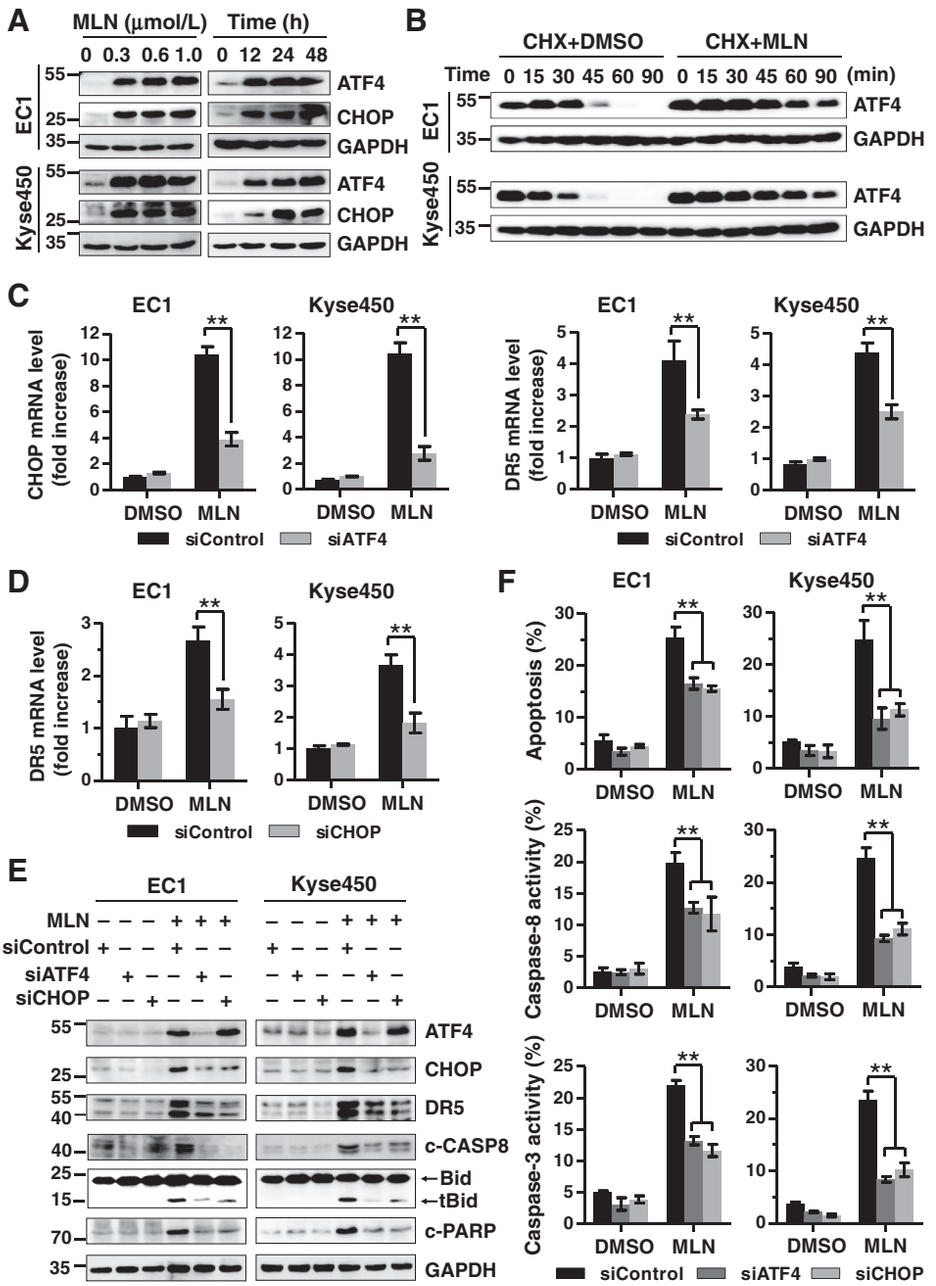

Figure 4.
ATF4 is responsible for MLN4924-induced apoptosis via the CHOP/DR5 pathway. **A,** MLN4924 enhanced the expression of ATF4 and CHOP. Cells were treated with MLN4924 at the indicated doses and time points. Cell extracts were prepared for IB analysis of ATF4 and CHOP. **B,** MLN4924 enhanced the protein stability of ATF4. Kyse450 and EC1 cells were pretreated with 0.6 μmol/L MLN4924 for 18 hours to increase the basal protein level of ATF4. Cells were then washed with PBS to remove residual drug and divided into two groups, which were further treated with 50 μg/mL cycloheximide (CHX) or CHX+MLN4924 (0.6 μmol/L) for indicated times and then collected for IB analysis. **C,** ATF4 transcriptionally regulated CHOP and DR5. Kyse450 and EC1 cells were transfected with control or ATF4 siRNA (48 hours), treated with 0.6 μmol/L MLN4924 (48 hours), and analyzed by qPCR (normalized to GAPDH). **D,** DR5 was transcriptionally regulated by CHOP. Kyse450 and EC1 cells were transfected with control or CHOP siRNA (48 hours), treated with 0.6 μmol/L MLN4924 (48 hours), and analyzed by qPCR (normalized to GAPDH). **E,** the expression of ATF4 and CHOP is responsible for MLN4924-induced apoptosis in ESCC cells by the ATF4/CHOP/DR5 pathway. Knockdown efficiency, CASP8 activation, and Bid and PARP cleavage were assessed by IB analysis. **F,** the expression of ATF4 and CHOP was critical for MLN4924-induced apoptosis in ESCC cells. Kyse450 and EC1 cells, transfected with control siRNA, ATF4, or CHOP siRNA, were further treated with 0.6 μmol/L MLN4924 for 48 hours. Apoptosis induction was quantified by Annexin V–FITC/PI double-staining analysis (top) or by enzymatic activity assay for CASP8 (middle) or CASP3 by FACS (bottom). All data were representative of at least three independent experiments (**, $P < 0.01$; $n = 3$; error bar, SD).

and B), we next determined whether MLN4924-induced Noxa expression was mediated by ATF4 in ESCC cells. As shown in Fig. 5E and F, downregulation of ATF4 fully inhibited the induction of Noxa at both mRNA (Fig. 5E) and protein levels (Fig. 5F) in EC1 and Kyse450 cells, demonstrating the importance of ATF4 in the transactivation of Noxa upon MLN4924 treatment.

Moreover, we found that the expression of ATF4, CHOP, DR5, and Noxa was also significantly induced by MLN4924 treatment in EC109, Kyse30, and Kyse510, other three ESCC cell lines (Supplementary Fig. S5C), which implied that inhibition of neddylation could induce a conserved apoptotic responses in ESCC cell lines.

Genetic inactivation of neddylation pathway via NAE1/UBA3 siRNA silencing recapitulates MLN4924-induced cytotoxic effects in ESCC cells

Our present data suggest that pharmaceutical inactivation of neddylation pathway with NAE inhibitor MLN4924 triggers ATF4/CHOP/DR5-mediated extrinsic apoptosis and ATF4/Noxa-mediated intrinsic apoptosis in ESCC cells. To further validate the role of neddylation inhibition in facilitating these cytotoxic effects of MLN4924, we inactivated neddylation by knocking down the expression of UBA3 and NAE1, two essential subunits of NAE heterodimer, via specific siRNAs and determined whether UBA3/NAE1 knockdown could recapitulate the cytotoxic

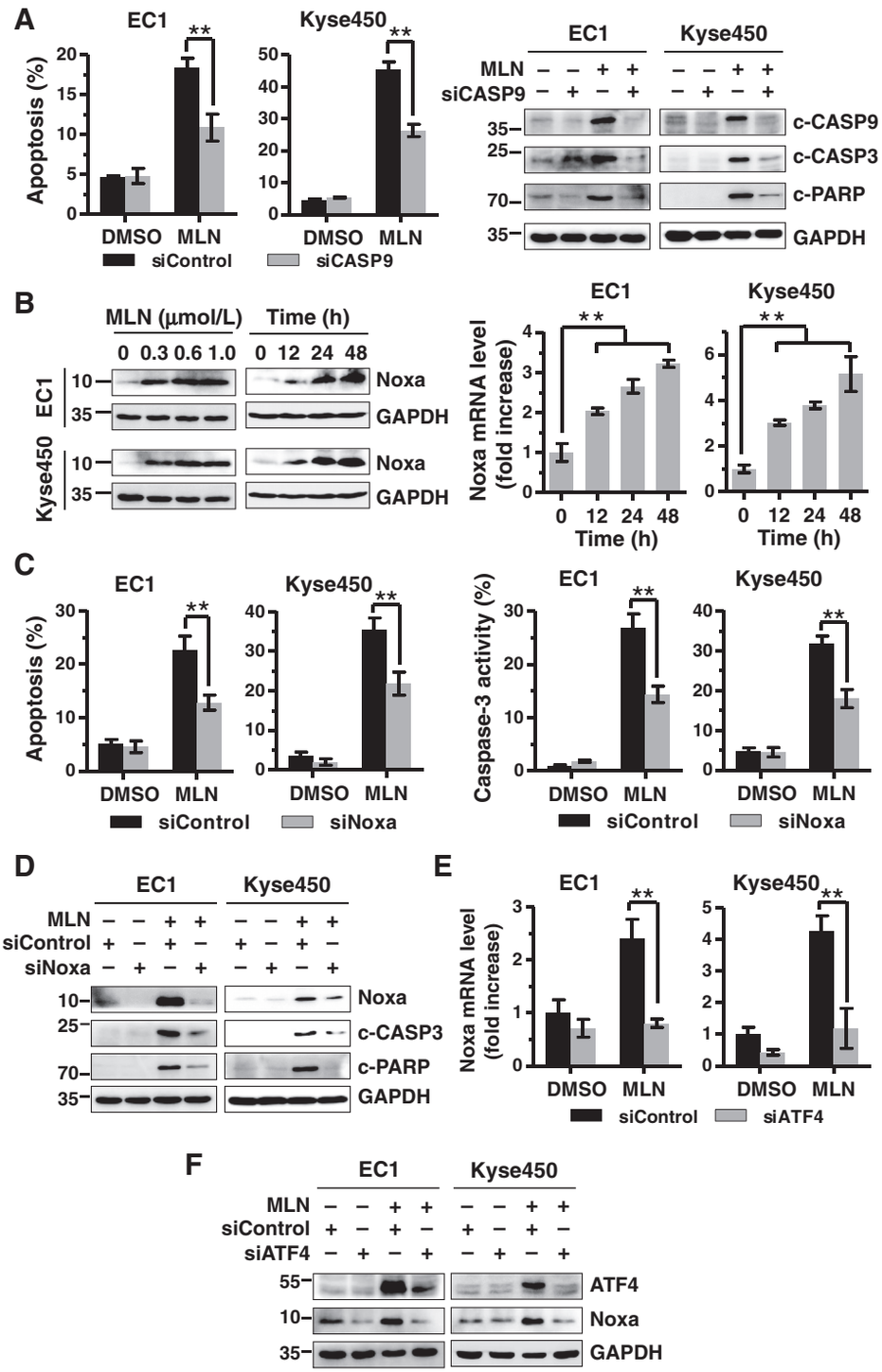

Figure 5.
Noxa is transactivated by ATF4 and participates in MLN4924-induced apoptosis in ESCC cells. **A,** CASP9 knockdown reduced MLN4924-induced apoptosis. Kyse450 and EC1 cells, transfected with siControl or siCASP9, were treated with MLN4924 (0.6 μmol/L) for 48 hours. Apoptosis was determined by the Annexin V–FITC/PI double-staining analysis (left). Cell lysates were collected and subjected to IB analysis for cleaved CASP3 and PARP. GAPDH served as a loading control (right). **B,** MLN4924 increased the expression of Noxa at both mRNA and protein levels. Kyse450 and EC1 cells were treated with MLN4924 (0.6 μmol/L) at the indicated concentrations and time. Cell extracts were prepared, and equal amounts of protein were loaded and separated by SDS-PAGE and subjected to IB analysis with anti-Noxa antibody. GAPDH served as a loading control (left). The mRNA level of Noxa was determined by the qPCR assay (right). **C** and **D,** downregulation of Noxa reduced MLN4924-induced apoptosis. Kyse450 and EC1 cells were transfected with control siRNA or Noxa siRNA and then treated with 0.6 μmol/L MLN4924 for 48 hours. Apoptosis induction was quantified by Annexin V–FITC/PI double-staining analysis (**C,** left) or CASP3 activity analysis by FACS (**C,** right). Knockdown efficiency and cleaved PARP/CASP3 were assessed by IB analysis (**D**). **E** and **F,** ATF4 transcriptionally regulated Noxa. Kyse450 and EC1 cells were transfected (48 hours) with control or ATF4 siRNA, treated with 0.6 μmol/L MLN4924 (48 hours). Transcriptional regulation of ATF4 on Noxa was analyzed by qPCR (normalized to GAPDH; **E**). Knockdown efficiency and expression of Noxa were assessed by IB analysis (**F**). All data were representative of at least three independent experiments (**, $P < 0.01$; $n = 3$; error bar, SD).

effects of MLN4924. Similar to MLN4924 treatment, knockdown of UBA3 and NAE1 significantly impaired cell viability in both EC1 and Kyse450 cells (Supplementary Fig. S6A). Moreover, UBA3/NAE1 siRNA silencing also induced apoptosis, as evidenced by the increased Annexin V–positive cells (Supplementary Fig. S6B), appearance of typical apoptotic morphology (Supplementary Fig. S6C), and the induction of cleaved fragments of CASP8, CASP9, CASP3, and PARP (Supplementary Fig. S6D) in treated cells, indicating the induction of extrinsic and intrinsic apoptosis. Like MLN4924, knockdown of UBA3 and NAE1 also upregulated the expression of ATF4, CHOP, and DR5 as well as Noxa (Supplementary Fig. S6D) in both EC1 and Kyse450 cell

lines. These results demonstrate that genetic inactivation of neddylation pathway via NAE1/UBA3 siRNA silencing fully recapitulates MLN4924-induced apoptosis activation in ESCC cells.

MLN4924 suppresses the growth of human ESCC tumors in murine model

After demonstrating the anticancer efficacy of MLN4924 *in vitro*, we further investigated the therapeutic potential of MLN4924 in subcutaneous-transplantation tumor model of human esophageal cancer in mice. To determine tumor growth in real time by external and noninvasive whole-body fluorescent optical imaging, EC1 cells expressing GFP (EC1-GFP) cells were implanted subcutaneously in mice (32, 33). MLN4924 treatment significantly suppressed tumor growth over time, whereas control tumors grew rapidly, as revealed by real-time images of tumors (Fig. 6A), tumor growth

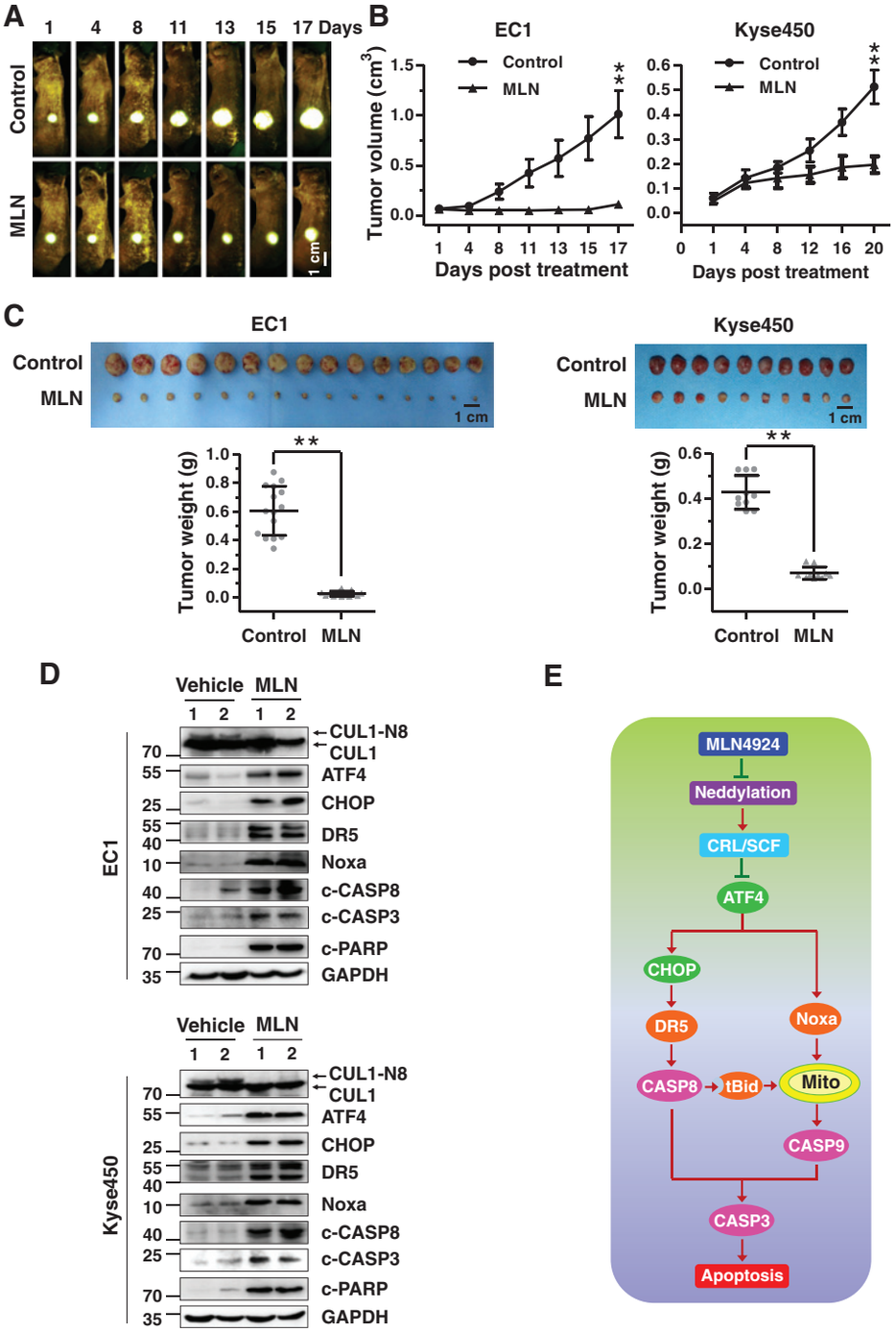

Figure 6.
MLN4924 suppressed esophageal tumor growth *in vivo*. Nude mice with subcutaneously transplanted human esophageal cancer cells EC1-GFP or Kyse450 were administrated with MLN4924 as indicated in Materials and Methods. **A,** whole-body images of EC1-GFP tumor model were captured twice a week. **B,** tumor size of both models was determined by caliper measurement, and the data were converted to tumor growth curves. **C,** mice were sacrificed and tumor tissues were harvested, photographed, and weighed at the end of study (**, $P < 0.01$; error bar, SD). **D,** proteins extracted from tumor tissues were analyzed by IB using anti-cullin1, ATF4, CHOP, DR5, cleaved CASP8/3/PARP, and Noxa antibodies. GAPDH was used as a loading control. **E,** schema of the mechanism for MLN4924-induced apoptosis in ESCC.

curve (Fig. 6B; **, $P < 0.01$), and tumor weight analysis (Fig. 6C; **, $P < 0.01$). Moreover, MLN4924 significantly inhibited the growth of established tumors (Fig. 6B and C) without obvious treatment-related toxicity, such as body weight loss (Supplementary Fig. S7). The *in vivo* anticancer effects of MLN4924 were further verified in another subcutaneous-transplantation tumor model using Kyse450 esophageal cancer cell line (Fig. 6B and C and Supplementary Fig. S7).

To address the potential mechanisms for the antitumor activity of MLN4924, we determined whether the ATF4/CHOP/DR5 axis was activated *in vivo*. As shown in Fig. 6D, MLN4924 completely inhibited cullin neddylation, indicating the inactivation of CRL/SCF E3 ligase. As the result, the expression of ATF4, CHOP, DR5, Noxa, and cleaved CASP8/CASP3/PARP was significantly induced by MLN4924 treatment (Fig. 6D). These observations indicated that MLN4924 inhibited esophageal tumor growth both *in vitro* and *in vivo* via the ATF4/CHOP/DR5/CASP8 extrinsic apoptosis and ATF4/Noxa intrinsic apoptosis pathways (Fig. 6E).

Discussion

Although researchers have made great efforts to understand the mechanistic basis for the initiation and progression of ESCC and to develop novel anti-ESCC strategies in the last decades, little achievements have been got in treatment of this deadly disease (23). In this study, we demonstrate that the entire neddylation pathway, including neddylation enzymes and global protein neddylation, was hyperactivated in ESCC and associated with poor overall survival of ESCC patients, indicating that the hyperactivated neddylation pathway may play an important role in tumorigenesis and tumor progression of ESCC. Moreover, inactivation of neddylation with investigational NAE inhibitor MLN4924, a first-in-class anticancer agent that is evaluated in several phase I/II clinical trials, demonstrated remarkable antitumor activity in ESCC tumors without observable side effect on body weight. These results indicate that protein neddylation pathway serves as an attractive anti-ESCC target.

Death receptor–mediated (extrinsic) apoptosis represents one of the most important cytotoxic pathways activated by anticancer agents (11, 27, 41–44). In this study, we demonstrated, to our knowledge for the first time, that neddylation inhibition with MLN4924 induces DR5-mediated apoptosis in ESCC cells. Mechanistic investigations further revealed that MLN4924-induced DR5 expression is transcription factors ATF4/CHOP-dependent, as evidenced by (i) MLN4924 stabilizes ATF4 as a CRL substrate to transactivate CHOP and DR5 sequentially to induce extrinsic apoptosis; and (ii) downregulation of ATF4 and CHOP expression via siRNA silencing significantly reduced DR5 transcription and attenuated MLN4924-induced apoptosis. Moreover, we found that DR5-mediated apoptosis is ligand-independent since downregulation of its cognate ligand TRAIL failed to rescue DR5-induced apoptosis. Similarly, it is reported that unmitigated ER stress induced CHOP-mediated DR5 transcription and CASP8-mediated apoptosis in a TRAIL-independent manner (27, 45). In addition, extrinsic apoptosis induced by MLN4924 in turn triggered intrinsic apoptosis through the CASP8/tBid axis. Collectively, these findings highlight induction of ATF4/CHOP/DR5-mediated extrinsic apoptosis as an important mechanism of MLN4924 action in ESCC cells (Fig. 6E). Moreover, this extrinsic apoptotic pathway may also be activated by MLN4924 treatment in other types of human cancer, which will be addressed in future studies.

BH3-only protein Noxa is a key mediator of intrinsic apoptosis (12, 46–48). MLN4924 was reported to induce Noxa expression and intrinsic apoptosis in several cancers, but the underlying mechanism for the induction of Noxa upon MLN4924 treatment remains largely unknown (3, 12, 22, 46). In the present study, we found that, in ESCC cells, MLN4924-induced Noxa is dependent on ATF4: first, MLN4924 blocks ATF4 turnover and induces its accumulation; second, the downregulation of ATF4 via siRNA silencing completely blocked the induction of Noxa. In support of our findings, endogenous ATF4 was demonstrated to bind to the Noxa promoter following treatment of cancer cells with several cytotoxic agents (40). Similarly, glutamine depletion in MYC-transformed cancer cells also induces apoptosis through ATF4-dependent Noxa and PUMA transactivation (49). Interestingly, Wang and colleagues reported that ATF3 can directly interact with ATF4 and cooperate with it to induce Noxa transactivation (39). Our unpublished data also show that MLN4924 treatment increases the expression of ATF3 in both mRNA and protein level, and knockdown of ATF3 downregulates the expression of Noxa. Future study will be performed to elucidate how ATF3 is transactivated by MLN4924 and how it interacts with ATF4 to regulate Noxa expression in esophageal cancer cells. In addition, during the preparation of this article, Knorr and colleagues reported that MLN4924 could cause accumulation of the CRL substrate c-Myc to transactivate Noxa and trigger intrinsic apoptosis in acute myelogenous leukemia cells (50), indicating cell-type–specific mechanisms for the induction of Noxa expression upon MLN4924 treatment.

Collectively, this study reveals induction of DR5-mediated extrinsic apoptosis as a previously unreported mechanism for neddylation-targeted anti-ESCC therapy. Our findings not only provide new insight into the cytotoxic action of neddylation inhibitors (e.g., MLN4924) in human cancer but also provide strong impetus for the clinical investigation of MLN4924 for the treatment of ESCC, a treatment-resistant disease with neddylation overactivation.

Disclosure of Potential Conflicts of Interest

No potential conflicts of interest were disclosed.

Authors' Contributions

Conception and design: P. Chen, T. Hu, L. Jia

Development of methodology: P. Chen, Y. Liang, P. Li, X. Chen, J. Zhang, Y. Ma, Q. Hao

Acquisition of data (provided animals, acquired and managed patients, provided facilities, etc.): P. Chen, Y. Liang, J. Wang, P Zhang, S. Yang, H. Qi

Analysis and interpretation of data (e.g., statistical analysis, biostatistics, computational analysis): P. Chen, T. Hu, L. Jia

Writing, review, and/or revision of the manuscript: P. Chen, T. Hu, R.M. Hoffman, Z. Dong, L. Jia

Administrative, technical, or material support (i.e., reporting or organizing data, constructing databases): Y. Zhang, H. Zhao, J. Yu, L.S. Jeong, M. Yang, Z. Dong

Study supervision: L. Jia

Grant Support

This work was supported by National Basic Research Program of China (973 program, 2012CB910302), National Natural Science Foundation Grant of China (grant nos. 81001102, 81101894, 81572340, 81172092, and 81372196), the Program for Professor of Special Appointment (Eastern Scholar) at Shanghai Institutions of Higher Learning, "Shuguang Program"

supported by Shanghai Education Development Foundation (14SG07), Development Foundation for The Excellent Youth Scholars of Zhengzhou University, and Research Foundation of Education Bureau of Henan Province, China (grant no. 15A310024).

The costs of publication of this article were defrayed in part by the payment of page charges. This article must therefore be hereby marked *advertisement* in accordance with 18 U.S.C. Section 1734 solely to indicate this fact.

Received September 15, 2015; revised February 14, 2016; accepted March 7, 2016; published OnlineFirst March 16, 2016.

References

1. Zhao Y, Morgan MA, Sun Y. Targeting Neddylation pathways to inactivate cullin-RING ligases for anticancer therapy. Antioxid Redox Signal 2014;21:2383–400.
2. Soucy TA, Smith PG, Milhollen MA, Berger AJ, Gavin JM, Adhikari S, et al. An inhibitor of NEDD8-activating enzyme as a new approach to treat cancer. Nature 2009;458:732–6.
3. Li L, Wang M, Yu G, Chen P, Li H, Wei D, et al. Overactivated neddylation pathway as a therapeutic target in lung cancer. J Natl Cancer Inst 2014;106:dju083.
4. Xirodimas DP, Saville MK, Bourdon JC, Hay RT, Lane DP. Mdm2-mediated NEDD8 conjugation of p53 inhibits its transcriptional activity. Cell 2004;118:83–97.
5. McLarnon A. Cancer: Mdm2-regulated stabilization of HuR by neddylation in HCC and colon cancer–a possible target for therapy. Nat Rev Gastroenterol Hepatol 2012;9:4.
6. Xie P, Zhang M, He S, Lu K, Chen Y, Xing G, et al. The covalent modifier Nedd8 is critical for the activation of Smurf1 ubiquitin ligase in tumorigenesis. Nat Commun 2014;5:3733.
7. Russell RC, Ohh M. NEDD8 acts as a 'molecular switch' defining the functional selectivity of VHL. EMBO Rep 2008;9:486–91.
8. Zuo W, Huang F, Chiang YJ, Li M, Du J, Ding Y, et al. c-Cbl-mediated neddylation antagonizes ubiquitination and degradation of the TGF-beta type II receptor. Mol Cell 2013;49:499–510.
9. Gao Q, Yu GY, Shi JY, Li LH, Zhang WJ, Wang ZC, et al. Neddylation pathway is up-regulated in human intrahepatic cholangiocarcinoma and serves as a potential therapeutic target. Oncotarget 2014;5:7820–32.
10. Xu J, Li L, Yu G, Ying W, Gao Q, Zhang W, et al. The neddylation-cullin 2-RBX1 E3 ligase axis targets tumor suppressor RhoB for degradation in liver cancer. Mol Cell Proteomics 2015;14:499–509.
11. Blank JL, Liu XJ, Cosmopoulos K, Bouck DC, Garcia K, Bernard H, et al. Novel DNA damage checkpoints mediating cell death induced by the NEDD8-activating enzyme inhibitor MLN4924. Cancer Res 2013;73:225–34.
12. Godbersen JC, Humphries LA, Danilova OV, Kebbekus PE, Brown JR, Eastman A, et al. The Nedd8-activating enzyme inhibitor MLN4924 thwarts microenvironment-driven NF-kappaB activation and induces apoptosis in chronic lymphocytic leukemia B cells. Clin Cancer Res 2014;20:1576–89.
13. Lin JJ, Milhollen MA, Smith PG, Narayanan U, Dutta A. NEDD8-targeting drug MLN4924 elicits DNA rereplication by stabilizing Cdt1 in S phase, triggering checkpoint activation, apoptosis, and senescence in cancer cells. Cancer Res 2010;70:10310–20.
14. Milhollen MA, Narayanan U, Soucy TA, Veiby PO, Smith PG, Amidon B. Inhibition of NEDD8-activating enzyme induces rereplication and apoptosis in human tumor cells consistent with deregulating CDT1 turnover. Cancer Res 2011;71:3042–51.
15. Milhollen MA, Traore T, Adams-Duffy J, Thomas MP, Berger AJ, Dang L, et al. MLN4924, a NEDD8-activating enzyme inhibitor, is active in diffuse large B-cell lymphoma models: rationale for treatment of NF-{kappa}B-dependent lymphoma. Blood 2010;116:1515–23.
16. Nawrocki ST, Kelly KR, Smith PG, Espitia CM, Possemato A, Beausoleil SA, et al. Disrupting protein NEDDylation with MLN4924 is a novel strategy to target cisplatin resistance in ovarian cancer. Clin Cancer Res 2013;19:3577–90.
17. Nawrocki ST, Kelly KR, Smith PG, Keaton M, Carraway H, Sekeres MA, et al. The NEDD8-activating enzyme inhibitor MLN4924 disrupts nucleotide metabolism and augments the efficacy of cytarabine. Clin Cancer Res 2015;21:439–47.
18. Shah JJ, Jakubowiak AJ, O'Connor OA, Orlowski RZ, Harvey RD, Smith MR, et al. Phase I study of the novel investigational NEDD8-activating enzyme inhibitor pevonedistat (MLN4924) in patients with relapsed/refractory multiple myeloma or lymphoma. Clin Cancer Res 2016;22:34–43.
19. Sarantopoulos J, Shapiro GI, Cohen RB, Clark JW, Kauh JS, Weiss GJ, et al. Phase I study of the investigational NEDD8-activating enzyme inhibitor pevonedistat (TAK-924/MLN4924) in patients with advanced solid tumors. Clin Cancer Res 2016;22:847–57.
20. Liao H, Liu XJ, Blank JL, Bouck DC, Bernard H, Garcia K, et al. Quantitative proteomic analysis of cellular protein modulation upon inhibition of the NEDD8-activating enzyme by MLN4924. Mol Cell Proteomics 2011;10:M111009183.
21. Kim W, Bennett EJ, Huttlin EL, Guo A, Li J, Possemato A, et al. Systematic and quantitative assessment of the ubiquitin-modified proteome. Mol Cell 2011;44:325–40.
22. Wang Y, Luo Z, Pan Y, Wang W, Zhou X, Jeong LS, et al. Targeting protein neddylation with an NEDD8-activating enzyme inhibitor MLN4924 induced apoptosis or senescence in human lymphoma cells. Cancer Biol Ther 2015;16:420–9.
23. Torre LA, Bray F, Siegel RL, Ferlay J, Lortet-Tieulent J, Jemal A. Global cancer statistics, 2012. CA Cancer J Clin 2015;65:87–108.
24. Belkhiri A, El-Rifai W. Advances in targeted therapies and new promising targets in esophageal cancer. Oncotarget 2015;6:1348–58.
25. Luo Z, Yu G, Lee HW, Li L, Wang L, Yang D, et al. The Nedd8-activating enzyme inhibitor MLN4924 induces autophagy and apoptosis to suppress liver cancer cell growth. Cancer Res 2012;72:3360–71.
26. Chen P, Hu T, Liang Y, Jiang Y, Pan Y, Li C, et al. Synergistic inhibition of autophagy and neddylation pathways as a novel therapeutic approach for targeting liver cancer. Oncotarget 2015;6:9002–17.
27. Wang G, Wang X, Yu H, Wei S, Williams N, Holmes DL, et al. Small-molecule activation of the TRAIL receptor DR5 in human cancer cells. Nat Chem Biol 2013;9:84–9.
28. Alves NL, Derks IA, Berk E, Spijker R, van Lier RA, Eldering E. The Noxa/Mcl-1 axis regulates susceptibility to apoptosis under glucose limitation in dividing T cells. Immunity 2006;24:703–16.
29. Yamaguchi H, Wang HG. CHOP is involved in endoplasmic reticulum stress-induced apoptosis by enhancing DR5 expression in human carcinoma cells. J Biol Chem 2004;279:45495–502.
30. Liu X, Yue P, Zhou Z, Khuri FR, Sun SY. Death receptor regulation and celecoxib-induced apoptosis in human lung cancer cells. J Natl Cancer Inst 2004;96:1769–80.
31. Ohoka N, Yoshii S, Hattori T, Onozaki K, Hayashi H. TRB3, a novel ER stress-inducible gene, is induced via ATF4-CHOP pathway and is involved in cell death. EMBO J 2005;24:1243–55.
32. Hu T, Qi H, Li P, Zhao G, Ma Y, Hao Q, et al. Comparison of GFP-expressing imageable mouse models of human esophageal squamous cell carcinoma established in various anatomical sites. Anticancer Res 2015;35:4655–63.
33. Hoffman RM. The multiple uses of fluorescent proteins to visualize cancer in vivo. Nat Rev Cancer 2005;5:796–806.
34. Lassot I, Segeral E, Berlioz-Torrent C, Durand H, Groussin L, Hai T, et al. ATF4 degradation relies on a phosphorylation-dependent interaction with the SCF(betaTrCP) ubiquitin ligase. Mol Cell Biol 2001;21:2192–202.
35. Emanuele MJ, Elia AE, Xu Q, Thoma CR, Izhar L, Leng Y, et al. Global identification of modular cullin-RING ligase substrates. Cell 2011;147:459–74.
36. Xu L, Su L, Liu X. PKCdelta regulates death receptor 5 expression induced by PS-341 through ATF4-ATF3/CHOP axis in human lung cancer cells. Mol Cancer Ther 2012;11:2174–82.
37. Martin-Perez R, Palacios C, Yerbes R, Cano-Gonzalez A, Iglesias-Serret D, Gil J, et al. Activated ERBB2/HER2 licenses sensitivity to apoptosis upon

endoplasmic reticulum stress through a PERK-dependent pathway. Cancer Res 2014;74:1766–77.
38. Han J, Back SH, Hur J, Lin YH, Gildersleeve R, Shan J, et al. ER-stress-induced transcriptional regulation increases protein synthesis leading to cell death. Nat Cell Biol 2013;15:481–90.
39. Wang Q, Mora-Jensen H, Weniger MA, Perez-Galan P, Wolford C, Hai T, et al. ERAD inhibitors integrate ER stress with an epigenetic mechanism to activate BH3-only protein NOXA in cancer cells. Proc Natl Acad Sci U S A 2009;106:2200–5.
40. Armstrong JL, Flockhart R, Veal GJ, Lovat PE, Redfern CP. Regulation of endoplasmic reticulum stress-induced cell death by ATF4 in neuroectodermal tumor cells. J Biol Chem 2010;285:6091–100.
41. Liu X, Yue P, Chen S, Hu L, Lonial S, Khuri FR, et al. The proteasome inhibitor PS-341 (bortezomib) up-regulates DR5 expression leading to induction of apoptosis and enhancement of TRAIL-induced apoptosis despite up-regulation of c-FLIP and survivin expression in human NSCLC cells. Cancer Res 2007;67:4981–8.
42. Miller CP, Ban K, Dujka ME, McConkey DJ, Munsell M, Palladino M, et al. NPI-0052, a novel proteasome inhibitor, induces caspase-8 and ROS-dependent apoptosis alone and in combination with HDAC inhibitors in leukemia cells. Blood 2007;110:267–77.
43. Brooks AD, Jacobsen KM, Li W, Shanker A, Sayers TJ. Bortezomib sensitizes human renal cell carcinomas to TRAIL apoptosis through increased activation of caspase-8 in the death-inducing signaling complex. Mol Cancer Res 2010;8:729–38.
44. Nagalingam A, Kuppusamy P, Singh SV, Sharma D, Saxena NK. Mechanistic elucidation of the antitumor properties of withaferin a in breast cancer. Cancer Res 2014;74:2617–29.
45. Lu M, Lawrence DA, Marsters S, Acosta-Alvear D, Kimmig P, Mendez AS, et al. Cell death. Opposing unfolded-protein-response signals converge on death receptor 5 to control apoptosis. Science 2014;345:98–101.
46. Dengler MA, Weilbacher A, Gutekunst M, Staiger AM, Vohringer MC, Horn H, et al. Discrepant NOXA (PMAIP1) transcript and NOXA protein levels: A potential Achilles' heel in mantle cell lymphoma. Cell Death Dis 2014;5:e1013.
47. Nikiforov MA, Riblett M, Tang WH, Gratchouck V, Zhuang D, Fernandez Y, et al. Tumor cell-selective regulation of NOXA by c-MYC in response to proteasome inhibition. Proc Natl Acad Sci U S A 2007;104:19488–93.
48. Nawrocki ST, Carew JS, Maclean KH, Courage JF, Huang P, Houghton JA, et al. Myc regulates aggresome formation, the induction of Noxa, and apoptosis in response to the combination of bortezomib and SAHA. Blood 2008;112:2917–26.
49. Qing G, Li B, Vu A, Skuli N, Walton ZE, Liu X, et al. ATF4 regulates MYC-mediated neuroblastoma cell death upon glutamine deprivation. Cancer Cell 2012;22:631–44.
50. Knorr KL, Schneider PA, Meng XW, Dai H, Smith BD, Hess AD, et al. MLN4924 induces Noxa upregulation in acute myelogenous leukemia and synergizes with Bcl-2 inhibitors. Cell death and differentiation 2015;22:2133–42.